Aus dem Department für Pathobiologie
der Veterinärmedizinischen Universität Wien

Institut für Immunologie
(Leiter: Univ.-Prof. Dr.rer.nat. Armin Saalmüller)

Lymphocyte Clonality Testing in Feline Intestinal Lymphoplasmacytic Infiltration: Friend or Foe?

Diplomarbeit

Veterinärmedizinische Universität Wien

vorgelegt von
Julia Huber

Wien, im Jänner 2021

Betreuerin: Dr.rer.nat. Sabine Hammer

Gutachterin: Ass.-Prof. Dr.med.vet. Nicole Luckschander-Zeller

DACVIM-CA DECVIM-CA

Danksagung

Zuallererst möchte ich mich bei Dr. Birgitt Wolfesberger von der Klinik für Interne Medizin Kleintiere (Vetmeduni Vienna) dafür bedanken, dass sie meiner beharrlichen Anfrage bezüglich einer Diplomarbeit nachgekommen ist, mich mit dem Thema vertraut gemacht und mich Dr. Sabine Hammer vom Institut für Immunologie (Vetmeduni Vienna) vorgestellt hat.

Bei Dr. Sabine Hammer möchte ich mich für ihre große Unterstützung, die immer raschen Antworten auf meine Hilferufe, die konstruktiven Gespräche und ihre Geduld bezüglich des Werdegangs dieser Diplomarbeit bedanken.

Weiters gilt mein Dank Dr. Andrea Fuchs-Baumgartinger vom Institut für Pathologie (Vetmeduni Vienna), die mich in allen histopathologischen Fragen und Belangen sehr mit ihrer Arbeit unterstützt hat.

Ein großes Dankeschön auch an Nora Nedorost vom Institut für Pathologie (Vetmeduni Vienna), die mir bei der DNA-Extraktion meiner Proben im Labor mit Rat und Tat zur Seite gestanden ist.

Danke liebe Mama, lieber Papa und lieber Andreas, die ihr ganz unterschiedlich und auf gleiche Weise unverzichtbar zu dieser Diplomarbeit und damit meinem Studienabschluss beigetragen habt.

Table of content

1. Introduction

1.1. Feline gastrointestinal diseases

The two main diseases of the feline gastrointestinal system are the lymphocytic-plasmacytic (inflammatory) enteropathy and the small cell lymphoma (Marsilio et al. 2020, Sabattini et al. 2016). Middle aged and elderly feline patients are most commonly afflicted and present with various and unspecific gastrointestinal symptoms (*e.g.* diarrhoea, vomiting or anorexia) (Jergens 2012). A differentiation of severe cases of mucosal lymphocytic-plasmacytic inflammation from a low grade small cell lymphoma can be difficult (Uzal et al. 2016).

1.1.1. Inflammatory bowel disease (IBD)

IBD represents a form of chronic enteropathy and is a loose term for any chronic gastrointestinal disorder with histopathologic signs of inflammation, such as lymphocytic-plasmacytic infiltration of the *Lamina propria mucosae* (Uzal et al. 2016, Washabau et al. 2010). Usually, IBD is a diagnosis of exclusion: (a) The patients' gastrointestinal symptoms must persist for more than three weeks, (b) inflammation of the mucosa must be evident in the histopathological examination, (c) infections with viruses and parasites must be ruled out as well as extraintestinal diseases (*e.g.* chronic kidney disease) and (d) there has to be insufficient response to dietary changes or antibiotic treatment (Jergens et al. 1992, Jergens 1999, Jergens 2012). The common and effective treatment with immunosuppressive agents, such as corticoids, suggests that excessive immune response plays a central role in the pathogenesis of IBD (Jergens 1999). This could be due to altered interactions between the faecal microbiome and the host's intestinal mucosa (Marsilio et al. 2019a). However, the actual underlying cause for IBD remains yet unknown.

1.1.2. Intestinal layers and local immune cells

The small intestine comprises of the duodenum, jejunum and ileum. The main function of the intestine is digestion, but apart from that, the intestinal mucosa plays a major role as the body's largest lymphatic organ (Liebich and Budras 2010).

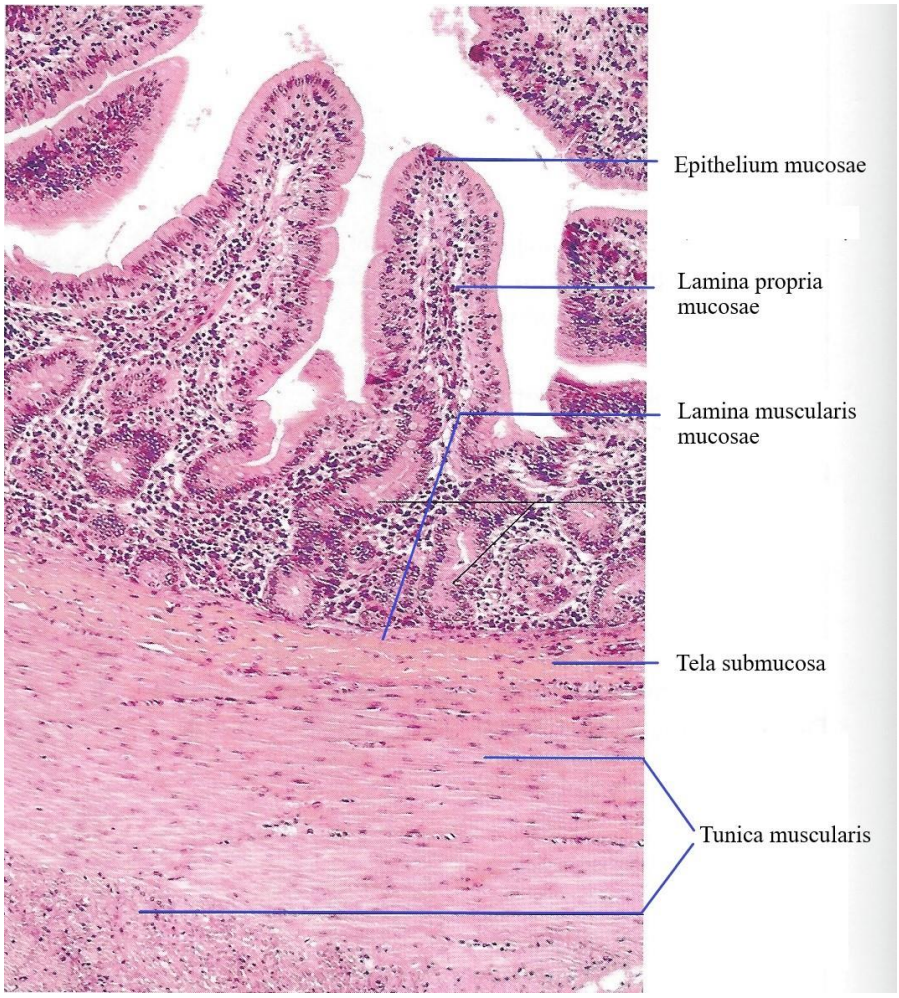

Fig 1: The intestinal layers of the jejunum (Liebich and Budras 2010).

The luminal layer, the *Tunica mucosa*, divides into three parts: *Epithelium mucosae*, *Lamina propria mucosae* and the outmost *Lamina muscularis mucosae* (compare ***Fig 1***). *Plicae circulares* and *Villi intestinales* are part of the *Tunica mucosa*. These folds and villi provide a larger surface area for digestive processes (Liebich and Budras 2010). Sometimes, a population of large granular lymphocytes (LGL) are detected in cats' intestinal *Tunica mucosa*; these cells show a specific eosinophilic granulation, which suggests a cytotoxic function. While they do not seem to increase in number in case of feline inflammatory enteropathy, there are observations of neoplastic events within this population (Konno et al. 1994, Roccabianca et al. 2000). Within the *Lamina propria mucosae* there are numerous lymphatic cells to provide defence function: T- and B-lymphocytes, plasma cells, monocytes, macrophages and mast cells

as well as eosinophils. They are referred to as gut-associated lymphoid tissue (Liebich and Budras 2010).

The *Tela submucosa* follows the *Tunica mucosa* and contains a variety of lymphonoduli, nerval plexus, blood vessels and fat tissue. The *Tunica muscularis* and the *Tunica serosa* form the outmost layers of the intestinal wall (Liebich and Budras 2010).

For standardised histopathologic evaluation of gastrointestinal inflammation the World Small Animal Veterinary Association (WSAVA) published guidelines in 2008 (Day et al. 2008). In 2010 the WSAVA International Gastrointestinal (GI) Standardization Group published an American College of Veterinary Internal Medicine (ACVIM) Consensus Statement. The GI Standardization Group recommends the following: (1) Endoscopy and intestinal biopsy are not indicated for every patient and therapeutic approaches are more effective in diagnosing antibiotic- and dietary-responsive forms of gastrointestinal inflammation. When, however, endoscopy is performed, biopsy should ideally be taken from the ileum. (2) IBD cannot be diagnosed by histopathology alone and should additionally be defined regarding clinical, pathogenetic, imaging, pathophysiologic and genetic criteria. (3) Clinicians who perform endoscopy should use standard report forms for documentation and examination. (4) Pathologists should assess tissue quality and quantity and (5) use a standardised classification system for evaluation of gastrointestinal tissue samples, as published by Day et al. (2008).

1.2. Feline alimentary lymphoma

Lymphomas are among the most frequently encountered tumours in both dogs and cats. They originate from the lymphatic tissue and thus from lymphatic cells, such as lymphocytes and lymphoblasts. Approximately 33 % of tumours occurring in cats are haematopoietic tumours, the majority of those being malignant lymphomas (Moore et al. 2012, Vail et al. 1998).

They can be classified by their anatomical site on one hand and by their cytological and histopathological appearance on the other. The anatomical classification is based on a modified model of the World Health Organisation (WHO) and differentiates between peripheral, mediastinal, gastrointestinal/alimentary, extranodal lymphoma and leukaemia (Hardy 1981). Alimentary lymphoma can occur in the upper or lower gastrointestinal tract, the liver or the pancreas with or without involvement of the regional lymph nodes (Lingard et al. 2009). The

alimentary lymphoma is the most common type of lymphoma in cats (Vail et al. 1998) and occurs most frequently in the small intestine (Pohlman et al. 2009).

Morphologic and immunohistologic criteria were taken into account to describe various types of B-, T- and natural killer (NK) cell lymphomas by the Revised European American Lymphoma (REAL) Classification for Domestic Animals, which was the basis for the classification of hematopoietic tumours in domestic animals published by the WHO (Valli et al. 2002).

Various potential causes for alimentary lymphomas are under discussion: Infections with feline retroviruses, such as feline leukaemia virus and feline immunodeficiency virus have been commonly associated with lymphoma (Beatty 2014). They are major risk factors although cats with alimentary lymphoma are usually tested negative for both viruses (Louwerens et al. 2005). According to the results of a study by Bridgeford and co-workers *Helicobacter heilmannii* can be associated with the development of feline gastric lymphoma. In *Helicobacter heilmannii*-infected humans antibiotic treatment resolved the concurrent mucosa associated lymphoid tissue (MALT) lymphoma, hence the hypothesis that feline gastric lymphoma patients could respond similarly (Bridgeford et al. 2008). Another risk factor for developing lymphoma is exposure to cigarette smoke (Bertone et al. 2002). It is also discussed that present chronic gastrointestinal inflammation can precede and accompany the development of alimentary lymphoma (Briscoe et al. 2011, Kiupel et al. 2011, Lingard et al. 2009, Moore et al. 2012).

The clinical condition of feline lymphoma patients depends on the tumour's location and type of lymphoma and includes unspecific symptoms such as anorexia, weight loss, diarrhoea and vomiting (Mahony et al. 1995).

Reliable diagnosis of alimentary lymphoma proves to be difficult and various approaches are currently available. With an ultrasound-guided fine needle aspiration biopsy cell material is gained from a suspicious intestinal mass or enlarged mesenteric lymph nodes for cytological examination. This can confirm the presence of alimentary lymphoma but is not suitable to grade and classify the type of lymphoma. In addition, the presence of inflammation may complicate a definitive diagnosis. Therefore, a full thickness biopsy taken surgically under general anaesthesia and sent for histopathological examination will provide better results than endoscopically obtained intestinal biopsies, which do not include all layers of the intestinum (Evans et al. 2006).

The differentiation between a severe lymphocytic inflammation and a small cell lymphoma of the intestine can be difficult in histopathology alone (Kiupel et al, 2011). A further step for the assessment of the infiltrating lymphocytes can be immunophenotyping. Immunohistochemistry allows to differentiate between B- and T-cell lymphoma and to detect their proportional distribution. An even distribution of both lymphocyte types makes inflammation more likely than lymphoma whereas an uneven distribution might hint towards either a B- or T-cell lymphoma (Gieger 2011, Marsilio 2020). A further diagnostic tool is the clonality testing. Clonality testing is a PCR based method to detect a clonal population of lymphocytes which indicates the presence of alimentary lymphoma, whereas a polyclonal (pc) expansion is typical for a mixed population of lymphocytes and characteristic for an inflammatory process such as IBD (Moore et al. 2005).

1.3. Clonality testing

Clonality testing, also known as polymerase chain reaction for antigen receptor rearrangement (PARR), is a widely used additional tool to differentiate between lymphoplasmacytic enteropathy and alimentary small cell lymphoma (Moore et al. 2005). With this method clonal B- or T-lymphocyte populations, that originate from a single neoplastic B- or T-cell, can be detected analysing the gene rearrangement of the B- and T-cell receptors (Gress et al. 2016, Hammer et al. 2017). Rout et al. (2019) developed a promising PARR assay for detecting immunoglobulin heavy chain (IGH) and T-cell receptor gamma (TCRG) rearrangements in feline lymphoid neoplasms. Their TCRG PARR assay had a specificity of 100 % and a sensitivity of 97 % under ideal conditions; the IGH PARR assay had a specificity of 98 % and a sensitivity of 87 %. Their assay was tested under ideal conditions with T-cell leukaemia representing T-cell neoplasms. With knowledge that diagnosis of alimentary lymphoma is often uncertain, they are planning in a next step to assess the diagnostic accuracy of PARR assay for feline samples from the gastrointestinal tract. A previous validation study by Hammer et al. (2017) regarding the test system used in this study showed a sensitivity of 70 % and a specificity of 90 %.

1.3.1. T-cell receptor gamma (TCRG)

The T-cell receptor (TCR) is a heterodimer and composed of two different protein chains. It is located on the surface of T-lymphocytes and works as an antigen recognition site. The two peptides are α and β or γ and δ chains resulting in αβ T-cells and γδ T-cells, respectively. Each of these chains (TCRα, TCRβ, TCRG and TCRδ) is encoded in a locus, a distinct region of a chromosome. At first, T-cells rearrange their TCRδ locus followed by TCRG, which results in a γδ T-lymphocyte. Some T-cells do not stop the process there and continue to rearrange their TCRβ and TCRα locus leading to an αβ phenotype (Blom et al. 1999). In this instance, the TCRδ locus is deleted (Rezuke et al. 1997), hence the TCRG locus can be used as the prime target for PARR as it remains present in both, αβ and γδ T-cells.

During early stages of lymphocyte differentiation unique clones of T-cell receptors develop on each T-cell due to rearrangement of TCR genes [variable (V), diversity (D), joining (J) and constant (C)] within the loci. A random recombination of V, D and J regions occurs, and diversity is further established by the deletion and insertion of randomly chosen nucleotides (Blom et al. 1999). The resulting junction is referred to as complementarity determining region 3 (CDR3). It determines the specificity of the TCR and represents the DNA region of interest that is amplified during PCR. The CDR3 amplicons differ in length when lymphocytes derive not from a single precursor cell but multiple cells as can be seen in reactive processes. In neoplastic processes on the other hand, all CDR3 amplicons have the same length because they originate from one single parental tumour cell (Langerak et al. 2012).

1.3.2. Immunoglobulin heavy chain (IGH)

The B-cell receptors are composed of three chains, which are encoded in one locus. Following a similar rearrangement principle as explained for the TCR, at first, the IGH locus is rearranged, directly followed by the immunoglobulin kappa light chain (IGK) locus. Some B-cells then proceed to rearrange their immunoglobulin lambda light chain (IGL) locus, which leads to the deletion of the IGK locus by rearrangement of the kappa-deleting element (KDE). Once the IGH locus has rearranged in both variants, it represents the main target for B-cell clonality testing. False negative results might occur due to somatic hypermutation, a physiological mechanism of mutation of antigen receptor gene during immune processes, which can affect primer binding in a negative way (Keller et al. 2016).

In B-cells, as well as in T-cells, the V, D, J and C genes are randomly recombined giving rise to the CDR3, which can be amplified during PCR. In neoplastic processes, CDR3 amplicons are of the same size, indicating that they originate from a single parental tumour cell. On the other hand, in reactive processes the CDR3 differs in length, which suggests multiple precursor cells (Langerak et al. 2012).

1.4. Objective

Current diagnostic conclusions for feline alimentary lymphoma include the patient's clinical symptoms, cytology, histopathology, immunohistochemistry and clonality testing.

In this study, we worked up formalin-fixed and paraffin-embedded (FFPE) tissue samples deriving from the small intestine of 34 cats. All of them showed signs of mild to moderate lymphoplasmacytic infiltration in histopathology.

Genomic DNA was extracted from the FFPE specimen, DNA concentration was determined and heavily fragmented genomic DNA (gDNA) samples, which would not be suitable for PCR, were excluded. In a next step, the antigen receptor rearrangement of the B- as well as the T-cell receptor were analysed by PCR and displayed using a specific software.

This study investigated how far histopathologically diagnosed cases of mild to moderate lymphoplasmacytic infiltration in feline patients correlate with the clonality tests.

2. Material and methods

2.1. Intestinal samples

The samples used in this retrospective study derived from the small intestine of cats and were originally collected through a biopsy in living cats or taken from dead cats at necropsy. To identify suitable samples for this diploma thesis, reports of the Institute of Pathology (Department of Pathobiology, University of Veterinary Medicine Vienna, Austria) within the database of the university, TIS ("Tierspitalinformationssystem"), were searched for the keywords "lymphoplasmacytic enteritis", "lymphoplasmacytic duodenitis" or "IBD" in feline patients; limited to the years 2007-2018. The FFPE tissue samples that matched the above criteria were taken from the archive of the Institute of Pathology. They were cut in 2 µm sections, stained with haematoxylin-eosin and immunohistochemistry was performed.

The assessment of the obtained samples was done according to the „Histopathological standards for the diagnosis of gastrointestinal inflammation in endoscopic biopsy samples from the dog and the cat" of the WSAVA International GI Standardization Group (Washabau et al. 2010). According to the WSAVA histopathological standards for inflammation of the duodenum, a mild increase in *Lamina propria* lymphocytes and plasma cells is defined as followed: Lymphocytes and plasma cells may occupy 25-50 % of the area of the villous *Lamina propria* in a x40 field; crypts may be separated by up to five lymphocytes or plasma cells. A moderate increase in *Lamina propria* lymphocytes and plasma cells is described as: Lymphocytes and plasma cells may occupy 50-75 % of the area of the villous *Lamina propria* in a x40 field; crypts may be separated by up to ten lymphocytes or plasma cells (Day et al. 2008).

2.2. Formalin-fixed and paraffin-embedded material

To obtain FFPE samples the tissues were immersed in a 4 % buffered formaldehyde solution corresponding to a 10 % neutral buffered formalin for 24 hours, to stop the natural process of decomposition. Afterwards, pieces of the fixed tissue are processed automatically in a tissue processor (Histokinette, Leica Biosystems, Vienna, Austria) to prepare the tissue for embedding in paraffin wax. After embedding, the sample can be sliced for either microscopic examination or further subsequent testing.

2.3. Immunohistochemistry

Immunohistochemistry was performed with a LabVision-Autostainer (Thermo Fisher Scientific, Fremont, USA) using the Bright Vision HRP- Polymer method. FFPE samples were cut in 2 µm sections, deparaffinized, rehydrated and pre-treated with heat (96 °C) in pH 6 citrate for 20 minutes for antigen unmasking. For blocking, endogenous peroxidase slides were incubated in Hydrogen Peroxidase Block (Thermo Fisher Scientific) for five minutes and to decrease background staining in Ultra Vision Protein Block (Thermo Fisher Scientific) for another ten minutes. A polyclonal rabbit anti-human antibody against CD3 (Dako, Glostrup, Denmark; diluted 1:1000) and a polyclonal rabbit anti-human antibody against CD20 (Spring Biosiences, diluted 1:1000) were used. The samples were incubated with the primary antibodies for 30 minutes, and subsequently with the secondary antibodies (Bright Vision poly HRP anti rabbit IgG, Immunologic, Duiven, Netherlands) for 30 minutes. For visualisation, DAB Quanto (Thermo Fisher Scientific) was used for five minutes. Next, the slides were counterstained with Mayer's haematoxylin, dehydrated, put into Neo-Clear and finally mounted in Neo-Mount (Merck, Darmstadt, Germany).

The prepared slides were examined by an experienced pathologist (Ass.-Prof. Dr.med.vet. Andrea Fuchs-Baumgartinger), who was blinded regarding the clonality results. The results are presented as estimated ratios of T- to B-lymphocytes. The respective number of cell nuclei positive for CD3 (T-lymphocytes) and CD20 (B-lymphocytes) occurring in the *Lamina propria mucosae* was estimated (Hammer et al. 2017). A ratio of 50:50 indicates a nearly even distribution of T- and B-lymphocytes.

2.4. Layer-associated lymphoplasmacytic infiltration

During the early stages of our study, we discovered more clonal results than expected. We therefore decided to establish a customized evaluation system extending the WSAVA standards to the *Tela submucosa*. As in a lymphocytic-plasmacytic inflammation the infiltration is usually confined to the *Lamina propria mucosae* and in lymphoma the cells often infiltrate beyond the mucosa (Kiupel et al., 2011) Thus, we wanted to provide an additional basis to compare and discuss our results. This layer-associated evaluation system was based on four categories (A, B, C and D). We differentiated between mild lymphoplasmacytic infiltration of the *Lamina propria mucosae* (A), mild lymphoplasmacytic infiltration of the *Lamina propria mucosae* and

the *Tela submucosa* (B), moderate lymphoplasmacytic infiltration of the *Lamina propria mucosae* (C) and moderate lymphoplasmacytic infiltration of the *Lamina propria mucosae* and the *Tela submucosa* (D).

2.5. Deparaffinization of the formalin-fixed, paraffin-embedded tissues

The deparaffinization as well as the DNA extraction followed the Standard Operating Procedure "Extraktion genomischer DNA aus Paraffin (Gewebe und Zellen)" of the Institute of Pathology (University of Veterinary Medicine Vienna, Austria).

The FFPE blocks were cut with a Microtome (Microm HM 400, VWR, Darmstadt, Germany) and the resulting 10 µm thin slices were put into 1.5 ml tubes (Eppendorf, Hamburg, Germany). Next, 1 ml of Xylol (SAV-Liquid Production GmbH, Flintsbach am Inn, Germany) was added to each tube, they were mixed thoroughly and then incubated for five minutes at room temperature. Afterwards, the tubes were centrifuged (Microcentrifuge, Eppendorf, Hamburg, Germany) for five minutes at 13,200 rpm. The resulting supernatant was removed using a pipette. These working steps, starting with the addition of Xylol to the tubes, were repeated for a second time. Next, 1 ml of Ethanol absolute (Merck, Darmstadt, Germany) was added to the tissue samples in the tubes and thoroughly mixed. The tubes were centrifuged for five minutes at 13,200 rpm and the supernatant was removed with a pipette. The washing procedure with Ethanol was repeated for a second time. Subsequently, the tubes were centrifuged for another minute at 13,200 rpm to remove the remaining Ethanol using a small volume pipette. Eventually, the tubes were opened and put into a desiccator for 30 minutes, for drying the tissue pellets in a vacuumed atmosphere.

2.6. DNA extraction

For the extraction of gDNA, the QIAamp® DNA Micro Kit (Qiagen, Hilden, Germany) was used and the working steps followed the manual "Isolation of Genomic DNA from Tissues" (QIAamp® DNA Micro Handbook, 12/2014; Qiagen).

For tissue lysis, 180 µl of Buffer ATL and 20 µl of Proteinase K were added to the dried pellets and the tubes were mixed by vortexing. The tubes were then placed onto a thermomixer (ThermoMixer F1.5, Eppendorf, Hamburg, Germany) for overnight incubation at 56 °C and

1200 rpm. In some cases, lysis was not yet completed and another 10 µl of Proteinase K had to be added, and incubation was continued until a homogenous solution was visible. The samples were then heated for one hour at 90 °C in the thermomixer to part possibly remaining crosslinks between the formalin and the gDNA. Next, the tubes were shortly centrifuged and cooled down to room temperature. Hereafter, 200 µl of Buffer AL was added and the samples were mixed thoroughly. Then, 200 µl of Ethanol was added to the tubes; they were mixed and incubated for five minutes at room temperature, and then centrifuged briefly. During the next step, the lysate was transferred to the corresponding QIAamp MiniElute columns, which in turn were placed in 2 ml collection tubes and then centrifuged for one minute at 13,200 rpm. The collection tubes - now containing the flow-through - were discarded and the MiniElute columns were put into new collection tubes. Afterwards, two similar washing steps were performed, starting with the addition of 500 µl of Buffer AW1 to the columns. Then the columns were centrifuged for one minute at 13,200 rpm. Again, the collection tubes were discarded along with the flow-through and the columns were placed into new collection tubes. These steps were identically repeated with Buffer AW2. Finally, the tubes were centrifuged for three minutes at 13,200 rpm to completely dry the membrane of the columns. Hereafter, the columns were transferred to 1.5 ml tubes and 100 µl of Buffer AE was pipetted to the centre of the membrane to elute the gDNA. After five minutes of incubation at room temperature the tubes were centrifuged for one minute at 13,200 rpm and the MiniElute columns were eventually discarded.

2.7. Determination of the genomic DNA concentration

To determine the concentration as well as the purity of the gDNA a full-spectrum, UV-Vis spectrophotometer (NanoDrop 2000c, Thermo Fisher Scientific, Waltham, Massachusetts, USA) was used. The device has a wavelength range from 190 to 840 nm and can measure sample volumes from 0.5 to 2 µl with high accuracy and reproducibility.

Nucleic acids have their absorption maximum at 260 nm. The absorption of the gDNA samples at 260 nm in comparison to 280 nm and 230 nm, respectively, gives two ratios (260/280 and 260/230). These indicate the purity and therefore quality of the gDNA. The 260/280 ratio should be around 1.8 (1.8-2.0). A lower value suggests a contamination of the sample with proteins, phenol or other compounds, which absorb at 260 nm. The 260/230 ratio ranges a bit higher, at

2.0-2.2. Here again, a value of less than 2.0 indicates contaminations of any kind, which have their absorption maximum at 230 nm.

The amount of absorbed light correlates positively with the concentration of DNA. For determining said concentration, the gDNA samples were measured at 260 nm and calculated by the software of the NanoDrop 2000c using Beer-Lambert law, which relates the absorption of light to the amount of nucleic acids. A DNA concentration above 50 ng/µl is considered desirable.

Before measuring the actual samples, a blank value had to be determined. 1.5 µl of Buffer AE (QIAamp DNA Micro Kit, Qiagen) was pipetted onto the lower measurement pedestal of the NanoDrop 2000c and the sampling arm was then lowered towards the pedestal. After the measurement, the sampling arm was raised again and both parts that met the buffer droplet were cleaned. The samples were measured in the same manner and at least in duplicates. If the results differed by more than 5 ng/µl a third measurement of the respective sample was performed.

2.8. PCR for antigen receptor gene rearrangement, Clonality testing

2.8.1. The feline androgen receptor (fAR)

Determination of gDNA concentration via UV-Vis measurement does not draw a conclusion for the sample's suitability for PCR. Therefore, a 189 bp fragment of the feline androgen receptor (fAR) gene served as an amplification control to rule out heavily fragmented gDNA. In cats, the androgen receptor gene transcript has a size of 2,712 bp and is located on the X-chromosome (Accession number XM_004000575). It is a member of the steroid hormone receptor superfamily and is expressed in various tissues (Chang et al. 1995).

The master mix for the fAR PCR assay consisted of 6.25 µl of TopTaq Master Mix (2x; containing TopTaq Polymerase, TopTaq PCR Buffer and desoxyribonucleoside triphosphate (dNTP); Qiagen), 0.25 µl fAR primer mix (50x), 150 ng of sample DNA and 5 µl of diethylpyrocarbonate-treated water (DEPC). One forward (fw) and one reverse (rev) primer were used in the fAR primer mix, both specifically targeting a 189 bp fragment the fAR gene:

AR/1+ fw: 5'-CACAATGCCGCTACGGGGACCT-3' and

AR/1- rev: 5'-AGGGGGTCACAGACCCTGACTCG-3' (Mochizuki et al. 2011).

The tubes were put into a thermal cycler (T-Professional, Biometra, Göttingen, Germany) and for initialisation of the PCR, a temperature of 95 °C was established for five minutes, to activate the DNA polymerase. The 95 °C were kept for another 30 seconds, which causes the denaturation of the gDNA by breaking the hydrogen bonds between the complementary bases. For 90 seconds the cycler lowered its temperature to 68 °C. In this step, the annealing of the primers to the now single stranded DNA takes place. The primer extension step lasted for 30 seconds at 72 °C. Free dNTPs were added to each other by the DNA polymerase to create a new DNA strand, which is complementary to the DNA template strand. The cycling steps two to four were repeated for 40 times, being followed by a final extension step for ten minutes at 68 °C, followed by the last step in which the cycler eventually cools down to 15 °C (compare ***Table 1***).

Table 1: PCR thermal cycling protocol.

initialisation	**95 °C**	**5 minutes**
40 cycles of	95 °C	30 seconds
	68 °C	90 seconds
	72 °C	30 seconds
final step	68 °C	10 minutes
	15 °C	forever

2.8.2. TCRG

For the TCRG PCR, three master mixes were prepared, each of which contains four forward primers targeting the V genes 1-5 and a primer mix composed of one reverse primer targeting a specific J gene (J1, J2, J3) (Mochizuki et al. 2012).

The mixture for the TCRG PCR assay consisted of 6.25 µl of Type-it Master Mix (2x; containing HotStarTaq Plus DNA Polymerase, Type-it Mutation Detect PCR Buffer and dNTP, Qiagen), 1.88 µl of Q-Solution (5x; Qiagen), 150 ng of gDNA sample, 0.25 µl of TCRG/V 50x fw primer mix, 0.25 µl of each one of the three reverse primers (TCRG/J1, TCRG/J2 and TCRG/J3) and 2.88 µl of DEPC.

Each primer set was run in triplicates accompanied by a positive and a non-template control (NTC). The positive control derives from the T-cell lymphoma cell line FT-1 (Mochizuki et al.

2012). The PCR reactions were run in a thermal cycler and with the cycling conditions as described in ***Table 1***.

The TCRG/V 50x fw primer mix contains four different forward primers targeting the variable (V) genes 1-5.

TCRG/V1-2 fw primer: 5'-GGSAGAAGAGCGACGAGGGCGTG-3'

TCRG/V3 fw primer: 5'-GGGCGAAGAGCGATGAGGGAGTG-3'

TCRG/V4 fw primer: 5'-GTAGTGAGGAGRATGCTGGTCTG-3'

TCRG/V5 fw primer: 5'-GGCAGAAGCATGACAAGGGCATG-3'

The three reverse primers target each of the three joining (J) genes 1-3.

TCRG/J1 rev primer: 5'-CCCTGAGCAGTGTGCCAGSAC-3'

TCRG/J2 rev primer: 5'-GGGGGAGTTACKATGASCTTARTTCC-3'

TCRG/J3 rev primer: 5'-ATCCAGATCTCAGGTTTGGGAGGAGG-3'

2.8.3. IGH

For the IGH PCR, three master mixes were prepared, each of which contains one forward primer targeting a specific V gene (V1F2, V3F3 and V3F4) and a primer mix composed of five reverse primers targeting the JH genes 1-5 (Mochizuki et al. 2011).

The three mixtures for the three different forward primers consisted of 6.25 µl of Type-it Master Mix (2x; containing HotStarTaq Plus DNA Polymerase, Type-it Mutation Detect PCR Buffer and dNTP, Qiagen), 1.88 µl of Q-Solution (5x; Qiagen), 150 ng of gDNA sample, 0.38 µl of JH 1-5 50x rev primer mix, 2.75 µl of DEPC and 0.25 µl of either V1F2 50x fw primer or V3F3 50x fw primer or V3F4 50x fw primer.

The three forward primers target each of the three variable (V) genes V1F2, V3F3 and V3F4.

V1F2 fw primer: 5'-GCAGACACATCCACAAACACAGCCTAC-3'

V3F3 fw primer: 5'-GGGTCCGCCAGGCTCCAGG-3'

V3F4 fw primer: 5'-GGCCGATTCACCATCTCCAGAGAC-3'

The JH 1-5 50x rev primer mix contains five different reverse primers targeting the joining (J) genes 1-5.

JH1 rev primer: 5'-GCYSTCACCAGGRYTCCYBGGC-3'

JH2 rev primer: 5'-GCTGYGACHMTDGTTCCAYGGCCC-3'

JH3 rev primer: 5'-GCGRTGAYCWGGGTRYCYTGGC-3'

JH4 rev primer: 5'-GCGGTGACCAGGGTCCCGGGGCCC-3'

JH5 rev primer: 5'-GCCGTCACCAGGGTTCCGACGCC-3'

Each primer set was run in triplicates accompanied by a positive control and a NTC. The positive control comes from the B-cell lymphoma cell line MS4 (Mochizuki et al. 2011). The PCR reactions were run in a thermal cycler and with the cycling conditions as described in ***Table 1***.

2.9. Data analysis (Gene Scanning)

The QIAxcel Advanced system (Qiagen) uses capillary electrophoresis to separate DNA samples entirely automated and can process up to 96 samples at once. The system consists of a 12-channel capillary electrophoresis instrument, a QIAxcel Kit, including a QIAxcel gel cartridge and reagents, a computer and QIAxcel ScreenGel Software.

The QIAxcel Advanced is set up with a gel cartridge, running and wash buffers and calibrated using intensity markers. For analysis, the samples are placed onto the sample plate holder. The data collection settings are then selected, and the samples pass through the capillaries of the gel cartridge. The final data analyses were executed by the corresponding software.

For operation of the QIAxcel Advanced System, the QIAxcel DNA High Resolution Kit (Qiagen) was used, which enables the analysis of DNA ranging from 15 bp to 5000 bp in size. The following reagents are included in the kit. QX Intensity Calibration marker calibrates the signal intensity for each new gel cartridge, QX DNA Separation Buffer allows the separation of DNA molecules, QX Wash Buffer prevents cross-contamination, QX Mineral Oil protects the samples from evaporating. Before initialising the run, 10 µl of QX DNA Dilution Buffer were added to each of the PCR reactions to optimize the sample concentration for the subsequent gel electrophoresis. The QX Alignment marker is used to adjust the migration time variation across all channels and consisted of 15 bp and 1000 bp fragments.

For each gel run, the QIAxcel ScreenGel Software produces an electropherogram ("trace") as well as idealized gel image formats. Data analysis is based on an algorithm that calculates a variety of peak features, such as peak height, width number and area. The exported data for

visualisation contained digital images of the electropherograms and a detailed summarising report of the experiment as a PDF file (QIAGEN GmbH 2017).

2.10. Data interpretation of clonality testing

The expected size of distinct peaks ranged from 100 to 300 bp. To obtain reproducibility of results, the primer sets were subjected to triplicate PCRs for each DNA sample. If the electropherograms differed amongst these triplicates, the sample was considered to be pseudoclonal (psc). A singular distinct peak in the expected size range was regarded as monoclonal (mc) (compare ***Fig 2a***). Two distinct peaks matching these criteria were interpreted as biclonal (bc), more than two as oligoclonal (oc). A distribution of peaks in a Gaussian manner was classified as polyclonal (pc) (compare ***Fig 2b***). In several cases, the monoclonal peak was accompanied by a polyclonal distribution of peaks, covering the expected size range for the specifically applied primer sets. Those patterns were considered as monoclonal with a polyclonal background (mc+bg).

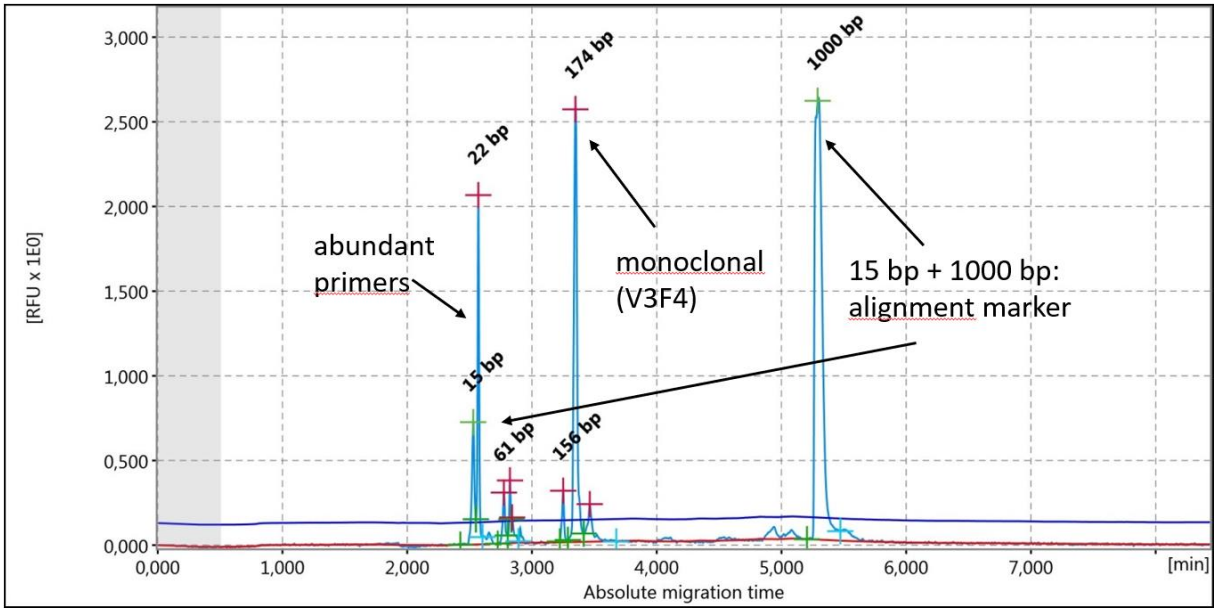

a)

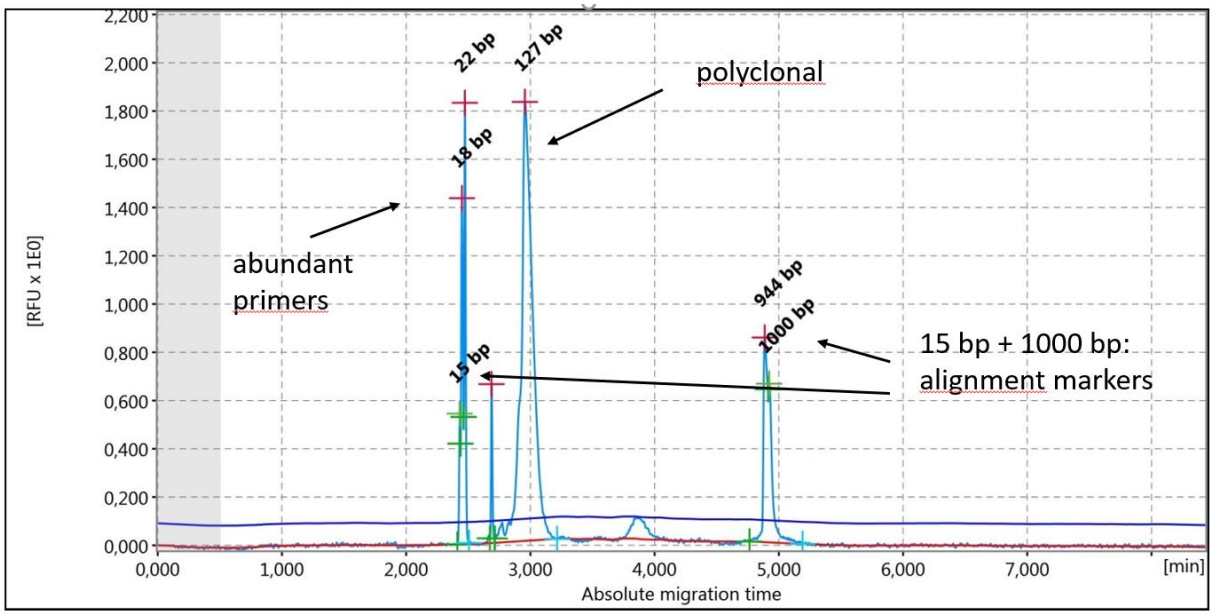

b)

Fig 2: Capillary electropherogram from clonality assays.
a) A single distant peak as shown in this electropherogram indicates a monoclonal result.
b) This curve represents a Gaussian distribution and is therefore considered a polyclonal pattern.

3. Results

3.1. Intestinal samples

The samples used in this retrospective study cover the years 2007 to 2018. In total, 34 feline intestinal biopsies had in common a histopathological diagnosis of a mild to moderate increase in *Lamina propria* lymphocytes and plasma cells matching to a mild to moderate lymphoplasmacytic infiltration**;** 22 samples had a mild increase in *Lamina propria* lymphocytes and plasma cells and 12 samples showed a moderate increase in lymphoplasmacytic infiltration. The highest number of patients being available from the years 2007 and 2014 (n = 6 each) as well as 2013 and 2017 (n = 5 each), respectively.

The ages of the cats at the point of diagnosis of lymphoplasmacytic infiltration ranged from 2 to 19 years (median, 10.7 years). The sex distribution was as follows: 12 spayed females, 4 females, 17 castrated males and 1 male. The breeds included 26 European Shorthair cats, 1 Chartreux, 1 Maine Coon, 1 Bengal, 1 Persian, 1 Ragdoll, 1 Egyptian Mau, 1 mixed and 1 undetermined breed (compare ***Table 2***).

Table 2: Breed, gender and age of the cats included in the present study.

Case ID	breed	gender	age	*Case ID*	breed	gender	age
1	Chartreux	mc	9 y	*18*	ESH	fs	12 y
2	ESH	fs	5 y	*19*	ESH	m	9 y
3	Maine Coon	mc	2 y	*20*	ESH	fs	10 y
4	ESH	mc	2 y	*21*	ESH	fs	11 y
5	ESH	mc	12 y	*22*	Ragdoll	mc	13 y
6	Bengal	f	10 y	*23*	n/d	fs	10 y
7	ESH	mc	5 y	*24*	mix	mc	13 y
8	Persian	fs	n/d	*25*	ESH	mc	10 y
9	ESH	f	7 y	*26*	ESH	mc	13 y
10	ESH	fs	19 y	*27*	ESH	fs	10 y
11	ESH	fs	17 y	*28*	ESH	f	15 y
12	ESH	fs	16 y	*29*	ESH	fs	7 y
13	ESH	mc	n/d	*30*	Egyptian Mau	mc	17 y
14	ESH	mc	12 y	*31*	ESH	fs	13 y
15	ESH	mc	10 y	*32*	ESH	f	12 y
16	ESH	mc	10 y	*33*	ESH	mc	11 y
17	ESH	mc	10 y	*34*	ESH	mc	14 y

ESH: European Shorthair, n/d: not determined, mc: male castrated, fs: female spayed, f: female, m: male, y: years

3.2. Genomic DNA concentration and quality of studied tissue samples

The DNA concentration was measured with the NanoDrop 2000c, a full spectrum, UV-Vis spectrophotometer. For successful further processing, the concentration of the gDNA samples should have a minimum of 30 ng/µl, which was the case for all samples being analysed in this study (compare ***Table 3***). The measured DNA concentration of the 34 samples varied between 47.20 ng/µl and 1604.30 ng/µl with a mean concentration of 543.91 ng/µl.

Two ratios, 260/280 nm and 260/230 nm, are indicating the purity and quality of the gDNA. The first one should range from 1.80 to 2.00, the latter from 2.00 to 2.20. A contamination of the sample lowers the values of either one or both ratios. The results of the 260/280 ratio ranged from 1.91 to 2.17 (mean: 1.99), which suggested good quality of gDNA (***Table 3***). The 260/230 ratio showed a variation from 1.59 to 2.31 and a mean of 2.19 (***Table 3***). Only three samples ranged under the generally recommended value of 2.00 for the 260/230 ratio, indicating the presence of contaminants, such as organic solvents.

Since the measurement of DNA concentration is not a specific quality control to determine whether the extracted DNA is suitable for PCR, a 189 bp fragment of the fAR gene was amplified using two gene specific primers. Samples with heavily fragmented gDNA do not amplify the fAR gene and would therefore lead to negative results in the capillary electrophoresis (QIAxcel Advanced System). In consequence, they should be excluded from further clonality testing to avoid ambiguous and therefore misleading results. In this study, all of the 34 samples were tested positive for the fAR gene amplification and were therefore further subjected to clonality testing.

Table 3: Age of sample, DNA concentration and quality (ratios) in comparison to the clonality results.

Case ID	Year	gDNA [ng/µl]	260/280	260/230	Clonality result
1	2018	248.30	1.98	2.23	T-cell
2	2018	103.00	2.10	2.24	n/d
3	2017	489.05	1.96	2.29	n/d
4	2017	145.20	2.03	2.31	n/d
5	2017	94.90	2.09	2.24	T-cell
6	2016	57.60	2.17	2.09	T-cell
7	2016	47.20	2.12	2.10	n/d
8	2016	897.75	2.00	2.30	T-cell
9	2016	489.25	2.17	2.29	T-cell
10	2015	1199.53	2.13	2.24	T-cell
11	2015	1350.60	2.02	2.25	n/d
12	2015	917.50	1.99	2.22	n/d
13	2014	994.90	2.01	2.18	n/d
14	2014	945.30	2.03	2.21	T-cell
15	2014	363.60	1.94	1.97	n/d
16	2014	265.05	2.02	2.24	n/d
17	2014	289.70	1.95	1.59	T-cell
18	2013	296.75	1.95	2.28	T-cell
19	2013	649.40	1.91	2.24	T-cell
20	2013	489.00	1.98	2.15	T-cell
21	2013	1604.30	1.98	2.24	T-cell
22	2013	694.33	2.00	2.27	T-cell
23	2012	630.95	1.95	2.20	T-cell
24	2012	226.60	1.96	2.20	T-cell
25	2011	1276.50	2.03	2.18	T-cell
26	2012	357.95	1.91	2.26	n/d
27	2010	387.55	1.92	2.17	T-cell
28	2008	722.70	1.96	2.22	T-cell
29	2007	81.35	1.98	2.21	T-cell
30	2007	397.80	1.94	1.86	T-cell
31	2007	548.85	1.94	2.28	T-cell
32	2007	508.40	1.29	2.28	T-cell
33	2007	141.80	1.99	2.27	T-cell
34	2007	580.35	1.93	2.24	n/d

n/d: not detected

3.3. Categories based on histopathology and immunohistochemistry

For better display and interpretation of the histopathological examination and immunohistochemistry results, we established four categories (A, B, C and D) for the layer-associated lymphoplasmacytic infiltration. Thus, we wanted to provide an additional basis to challenge the findings of the clonality testing approach. We assigned each sample to one of these groups, based on its lymphocytes' occurrence in the intestinal layers and the amount of cells found (compare ***Table 4***).

Table 4: Layer-associated lymphoplasmacytic infiltration.

Category	**Definition**	**Number of samples**
A	mild lymphoplasmacytic infiltration of the *Lamina propria mucosae*	15
B	mild lymphoplasmacytic infiltration of the *Lamina propria mucosae* and the *Tela submucosa*	7
C	moderate lymphoplasmacytic infiltration of the *Lamina propria mucosae*	7
D	moderate lymphoplasmacytic infiltration of the *Lamina propria mucosae* and the *Tela submucosa*	5

Immunohistochemistry was performed in order to detect both B- and T-lymphocytes and to show their distribution in the FFPE samples under investigation. Antibodies against CD20 and CD3 were used to identify the B- and T-lymphocytes, respectively. The samples were examined by an experienced pathologist and the results are presented as estimated ratios of T:B cells (compare ***Table 5***).

Table 5: Estimated T:B ratios in the layer-associated categories in comparison to the clonality results.

Case ID	Category	Estimated ratio of T:B lymphocytes	Clonality result
2	A	50/50	n/d
3	A	50/50	n/d
4	A	50/50	n/d
7	A	50/50	n/d
9	A	90/10	T-cell
11	A	50/50	n/d
12	A	50/50	n/d
14	A	50/50	T-cell
15	A	50/50	n/d
16	A	50/50	n/d
21	A	60/40	T-cell
24	A	50/50	T-cell
29	A	50/50	T-cell
31	A	50/50	T-cell
32	A	60/40	T-cell
13	B	60/40	n/d
18	B	90/10	T-cell
19	B	70/30	T-cell
22	B	60/40	T-cell
23	B	50/50	T-cell
25	B	50/50	T-cell
27	B	90/10	T-cell
1	C	60/40	T-cell
5	C	50/50	T-cell
17	C	80/20	T-cell
26	C	60/40	n/d
28	C	50/50	T-cell
30	C	50/50	T-cell
33	C	50/50	T-cell
6	D	50/50	T-cell
8	D	90/10	T-cell
10	D	60/40	T-cell
20	D	60/40	T-cell
34	D	90/10	n/d

n/d: not detected

Detailed information on the established groups according to the histopathology of the tissue samples, their age and T- and B-lymphocyte ratios (immunohistochemistry-derived data) together with their clonality results are presented in the appendix (compare ***Table 6***).

3.4. Clonality patterns

None of the 34 samples subjected to clonality testing showed clonal IGH gene rearrangements (appendix ***Table 6***).

As for the TCRG gene rearrangement, we found T-cell clonality in 23 of the 34 cat patients, 19 of the 23 samples were showing a monoclonal result. Four samples showed a biclonal peak. In category A, 46.67 % presented with T-cell clonality, whereas in categories B and C already 85.71 % of the samples were clonal. Category D contains 80.00 % clonal results. The remainder of the samples showed polyclonal (n = 9) as well as pseudoclonal (n = 2) patterns. Our findings correlate mostly positively with the histopathological evidence with respect to the estimated T:B ratios in the categories A to D. However, we would have expected less clonal results in category A given the fact that the *Lamina propria mucosae* was only mildly infiltrated with lymphocytes. In categories B and C, the percentage of samples showing T-cell clonality increased, matching the histopathological findings of either infiltration of the *Tela submucosa* additionally to superficial *Lamina propria mucosae* (category B) or increased, moderate, infiltration of *Lamina propriae mucosae* (category C). The sample material in category D presented with the highest rate of monoclonal results (4 out of 5), thus also being in concordance with a moderate lymphoplasmacytic infiltration of *Lamina propria mucosae* and *Tela submucosa*.

3.5. Immunohistochemistry results

In category A, the majority of the samples (80 %) showed an even distribution of T- and B-cells, which means a ratio of 50:50. In two cases, there were slightly more T- than B-cells (60:40) and one patient's immunochemistry result showed 90 % T-cells and only 10 % B-cells. In category B, we found higher ratios than in group A. Only two out of seven displayed 50:50 ratios, another two were distributed 60:40 and 90:10, respectively. One sample had a B:T ratio of 70:30. Category C presented with four out of seven 50:00 ratios, two 60:40 and one 80:20. In the last group, D, we found only one 50:50 ratio, but two 60:40 and 90:10, respectively.

In general, 19 of 34 samples showed an even distribution (50:50) of B- and T-lymphocytes and this ratio predominated additionally in categories A and C where a mild (A) and moderate (C) lymphoplasmacytic infiltration of the *Lamina propria mucosae* could be detected. In categories

B and D, the infiltration with lymphocytes continued to the *Tela submucosa* and in these categories the T:B ratios increased up to 90:10.

4. Discussion

We asked whether clonality testing was positive in cats, which had been diagnosed with mild to moderate lymphoplasmacytic infiltration. In more than a half of the tissue samples (23 out of 34), T-cell clonality was detected and the patients could be therefore suspicious for T-cell lymphoma. This outcome was surprising because based on histopathology alone none of these patients would have been diagnosed with lymphoma.

The mean age of the patients at the point of histopathological diagnosis of lymphoplasmacytic infiltration was 10.7 years, which accords with other studies. The most affected breed in this study is the European Shorthair cat, which can be explained by the high abundance of this breed among cat owners. Female and male cats were represented equally.

The results of the DNA concentration and quality did not correlate negatively with the age of the specimens, meaning that the eldest tissue samples from 2007 were not less in quality than the ones from 2017 or 2018. All specimens showed a gDNA concentration over the required minimum of 30 ng/µl and positively amplified the fAR gene. This shows that the protocol that was used for deparaffinization and extraction of the gDNA from the FFPE samples is suitable for subsequent PCR assays.

In the studied cohort, no B-cell clonality was detected, although 80 % of the samples showed an even distribution of T- and B-cells in immunohistochemistry. This could be explained by the fact that the studied samples originate from the small intestine where the occurrence of B-cell lymphoma in most parts is very unlikely (Moore et al. 2012).

With respect to T-cell clonality, 67.65 % of the cases showed a clonal expansion of T-cells. According to their T:B ratios, these 23 out of 34 feline patient samples were assigned to the categories B, C and D exhibiting lymphoplasmacytic infiltrations of the *Lamina propria mucosae* and in categories B and D also the *Tela submucosa*. In these categories, the T:B ratios ranged from 50:50 to a maximum of 90:10.

We did not expect to detect that many monoclonal results given the fact that the patients were diagnosed by histopathology with mild to moderate rated lymphoplasmacytic intestinal infiltration. This leads us to the known hypothesis that clonality must not necessarily indicate the presence of lymphoma (Hammer et al. 2017, Keller et al. 2016). Sometimes clonal expansion of lymphocytes can also be detected in benign cases in response to chronic intestinal

inflammatory processes, for instance due to pathogens (Kiupel et al. 2011). This leads to the development of clonal lymphocytic subpopulations addressing this specific pathogen (Keller et al. 2016). On the other hand, a severe inflammation that presents as a polyclonal lymphocyte population could mask lymphoma (Paulin et al. 2018).

Luckschander-Zeller and co-workers used clonality testing to distinguish between canine chronic enteropathy (CCE) and intestinal lymphoma. In 4 out of 35 CCE cases mono- or oligoclonal patterns could be detected with the TCRG primer sets and none of these cases showed histopathological evidence for lymphoma. All of the cases improved during therapy of CCE, which also suggests that clonal rearrangement can occur in inflammatory processes (Luckschander-Zeller et al. 2019).

Furthermore, there is a phenomenon called lymphocyte trafficking. It occurs in the small and large intestines to maintain intestinal immune homeostasis and help in regulation of inflammation (Habtezion et al. 2016). This mechanism could explain the lack of evidence of lymphoma in histopathology. The actual lymphoma is present in another part of the gastrointestinal tract and only trafficking lymphocytes present in the *Lamina propria* of the tissue sample were detected by PCR.

Another lymphoma study addressed clonality testing in 41 non-domestic felines. Again, eight samples showed a monoclonal pattern whereas histopathology diagnosed lymphoma in only three out of eight cases. These positive clonality results could be the result of an immune response due to neoplastic growth elsewhere and the consequential proliferation and migration of clonal lymphocytic subpopulations (Unterkreuter et al. 2020).

According to a similar study by Marsilio and co-workers clinically healthy cats showed abnormal histopathological results when applying the current WSAVA guidelines for diagnosis of gastrointestinal inflammation for intestinal biopsy samples (Day et al. 2008, Marsilio et al. 2019b) . Most of them had mild to moderate lymphoplasmacytic enteritis. More than half of the cats participating in this study showed clonal rearrangements of the TCRG and were therefore considered positive for small cell lymphoma. These results are very similar to our findings and give rise to questioning the interpretation guidelines. Together with the WSAVA guidelines, clonality testing was developed by studying mainly samples from very young and specific pathogen free cats. Maybe the interpretation of histopathology and also PARR has to be based on other standards than for “normal” cat population. Possibly mild to moderate

lymphoplasmacytic intestinal infiltration or a monoclonal PARR result must not necessarily be interpreted as a pathological finding in elderly, clinically healthy cats (Marsilio et al. 2019b).

In those cases with a positive clonality result, we could not detect significantly higher T:B lymphocyte ratios, although we would have expected a higher rate of T-lymphocytes being connected with T-cell clonality. This showed that immunohistochemistry does not provide information about gene rearrangements and clonality of the T-cell receptors. Therefore, clonality testing is essential to detect actual gene rearrangements of the TCRG.

A major drawback of this retrospective study is given to the fact that the diagnosis of feline inflammatory enteropathy could not be made in the first place as we had only the histopathological report describing an increased intestinal lymphoplasmacytic infiltration. We had no detailed case history or follow up for the studied patients. The study also suffers from lack of information about the clinical condition of the feline patients at the time when the biopsy was taken. Additionally we had no knowledge of potential therapy approaches and their outcome. Hence, a diagnostically conclusive interpretation of the clonality testing as well as the histopathological results is very limited. The results of retrospective studies regarding diagnosis of feline alimentary lymphoma in general and using clonality testing in particular are less conclusive because crucial patient data, especially the response to conservative treatment, are missing. Prospective studies are rare because the study design is much more elaborate, although prospective studies would give the correct interpretation and validity of clonality testing a push.

This study underlines the difficulties in interpreting positive clonality tests in feline patients with increased intestinal lymphoplasmacytic infiltration. This technique is far from being a stand-alone tool and the results have to be interpreted in a context with the patient's history, clinical status, histopathological examination and the clinical response to therapy. So far, a clonal result alone appears to be no final prove for the presence of alimentary lymphoma. Positive clonality patterns seem to occur regularly in cats with increased intestinal lymphoplasmacytic infiltration and the reasons for this are subject to further, preferably, prospective studies.

5. Zusammenfassung

In dieser Diplomarbeit gingen wir unter anderem der Frage nach, ob bei der Aufarbeitung von chronischen Darmerkrankungen bei der Katze die Klonalitätsprüfung eine geeignete alleinstehende diagnostische Methode darstellt. Die beiden häufigsten gastrointestinalen Erkrankungen bei der Katze sind einerseits die entzündliche Darmerkrankung („inflammatory bowel disease“, IBD) und andererseits das alimentäre Lymphom. Mittels Klonalitätsprüfung, einer PCR-basierten Methode, kann zwischen einer klonalen und einer heterogenen Lymphozytenpopulation unterschieden werden. Letzteres spricht eher für einen entzündlichen Prozess, während ersteres lymphomverdächtig ist.

In dieser retrospektiven Studie wurde das CDR3-Repertoire der B- und T-Zell-Rezeptoren mittels PCR analysiert. Hierfür wurden 34 in Formalin-fixierte und Paraffin-eingebettete Dünndarmproben von Katzen mit dem histopathologischen Befund „gering- oder mittelgradige lymphoplasmazelluläre Infiltration untersucht. Nach der DNA-Extraktion wurden Untersuchungen zur PCR-Tauglichkeit der Proben und anschließend die eigentliche Klonalitätsprüfung durchgeführt. Des Weiteren wurden eine erneute histopathologische sowie eine immunhistochemische Untersuchung durchgeführt.

Innerhalb der untersuchten Kohorte fanden wir in 23 der 34 Fälle ein klonales Ergebnis, wobei 19 Proben ein monoklonales Muster zeigten. Lymphoplasmazelluläre Entzündungen sind in der Regel auf die *Lamina propria mucosae* beschränkt. Lymphome, hingegen, können über die *Tunica mucosa* hinaus infiltrieren. Daher wurde weitergehend untersucht, ob eine Ausdehnung der gering- bis mittelgradigen lymphozytären Infiltration auf die *Tela submucosa,* ein Hinweis auf ein beginnendes Lymphom und damit eine Erklärung für die hohe Anzahl an klonalen Ergebnissen sein könnte. Anhand der histopathologischen Befunde wurden vier, die Darmschichten betreffende, Gruppen definiert, mithilfe derer die Ergebnisse der Klonalitätsprüfung dargestellt und diskutiert wurden (gering- und mittelgradige lymphoplasmazelluläre Infiltration der *Lamina propria mucosase* sowie gering- und mittelgradige lymphoplasmazelluläre Infiltration der *Lamina propria mucosae* und der *Tela submucosa*). Eine schlüssige Aussage konnte jedoch nicht gefunden werden.

Zusammenfassend lässt sich sagen, dass die Klonalitätsprüfung eine mögliche Methode in der Diagnostik von chronischen, felinen Darmerkrankungen ist, jedoch nicht als alleinstehender Test verwendet werden kann. Die Ergebnisse müssen immer in Kombination mit dem

klinischen Zustand des Tieres, der Krankengeschichte und der histopathologischen Untersuchung interpretiert werden.

6. Summary

In this diploma thesis, we focused on clonality testing in the diagnostic work-up of feline chronic enteropathy and asked whether it can be seen as a suitable stand-alone method. The two most common feline gastrointestinal diseases are the lymphoplasmacytic enteropathy and the alimentary small cell lymphoma. Clonality testing enables us to detect clonal B- or T-lymphocyte populations that originate from a single neoplastic B- or T-cell.

In this retrospective study, we analysed the CDR3 repertoire of the B- and T-cell receptors. Therefore, formalin-fixed, paraffin-embedded (FFPE) samples from the small intestine of 34 cats were selected. They all had in common a histopathological report of mild or moderate lymphoplasmacytic intestinal infiltration. After genomic DNA extraction and further PCR suitability tests, the feline patient samples were assayed by clonality testing, together with immunohistochemistry and histopathological examination.

In 23 out of 34 cases clonal results occurred, of which 19 showed a monoclonal pattern. As in a lymphocytic-plasmacytic inflammation, the infiltration is usually confined to the *Lamina propria mucosae* and in lymphoma, the cells often infiltrate beyond the mucosa. Therefore, the additional mild to moderate lymphoplasmacytic infiltration of the *Tela submucosa* was assessed to find out whether this suggests early lymphoma and thus explain the high number of monoclonal clonality results. Based on histopathology and immunohistochemistry, four layer-associated categories were established. The obtained clonality results were discussed as compared with the following categories: Mild and moderate lymphoplasmacytic infiltration of the *Lamina propria mucosae*, mild and moderate lymphoplasmacytic infiltration of the *Lamina propria mucosae* and *Tela submucosa*.

This study underlines that clonality testing can be used as an adjunct diagnostic approach in feline patients with chronic enteropathy. However, this technique is far from being a stand-alone tool and the obtained results have to be interpreted in the context with the patient's history, clinical status and histopathological examination.

7. Abbreviations

ACVIM	American College of Veterinary Internal Medicine
bc	biclonal
bp	base pair
CCE	canine chronic enteropathy
CDR3	complementarity determining region 3
DEPC	Diethylpyrocarbonate-treated water
dNTP	Desoxyribonucleoside triphosphate
ESH	European Shorthair
f	female
fAR	feline androgen receptor
FFPE	formalin-fixed and paraffin-embedded
fs	female spayed
gDNA	genomic DNA
GI	gastrointestinal
IBD	inflammatory bowel disease
IGH	immunoglobulin heavy chain
IGK	immunoglobulin kappa light chain
IGL	immunoglobulin lambda light chain
KDE	kappa-deleting element
LGL	large granular lymphocyte
m	male
MALT	mucosa associated lymphoid tissue
mc	male castrated
mc	monoclonal
mc+bg	monoclonal with background
n/d	not determined

n/d	not detected
NK	natural killer
NTC	non-template control
psc	pseudoclonal
REAL	Revised European American Lymphoma
TCR	T-cell receptor
TCRG	T-cell receptor gamma
TIS	Tierspitalinformationssystem
WHO	World Health Organisation
WSAVA	World Small Animal Veterinary Association

8. References

Beatty J. 2014. Viral causes of feline lymphoma: retroviruses and beyond. Veterinary journal (London, England: 1997), 201 (2): 174–180.

Bertone ER, Snyder LA, Moore AS. 2002. Environmental tobacco smoke and risk of malignant lymphoma in pet cats. American journal of epidemiology, 156 (3): 268–273.

Blom B, Verschuren MC, Heemskerk MH, Bakker AQ, van Gastel-Mol EJ, Wolvers-Tettero IL, van Dongen JJ, Spits H. 1999. TCR gene rearrangements and expression of the pre-T cell receptor complex during human T-cell differentiation. Blood, 93 (9): 3033–3043.

Bridgeford EC, Marini RP, Feng Y, Parry NMA, Rickman B, Fox JG. 2008. Gastric Helicobacter species as a cause of feline gastric lymphoma: a viable hypothesis. Veterinary immunology and immunopathology, 123 (1-2): 106–113.

Briscoe KA, Krockenberger M, Beatty JA, Crowley A, Dennis MM, Canfield PJ, Dhand N, Lingard AE, Barrs VR. 2011. Histopathological and immunohistochemical evaluation of 53 cases of feline lymphoplasmacytic enteritis and low-grade alimentary lymphoma. Journal of comparative pathology, 145 (2-3): 187–198.

Chang C, Saltzman A, Yeh S, Young W, Keller E, Lee HJ, Wang C, Mizokami A. 1995. Androgen receptor: an overview. Critical reviews in eukaryotic gene expression, 5 (2): 97–125.

Day MJ, Bilzer T, Mansell J, Wilcock B, Hall EJ, Jergens A, Minami T, Willard M, Washabau R. 2008. Histopathological standards for the diagnosis of gastrointestinal inflammation in endoscopic biopsy samples from the dog and cat: a report from the World Small Animal Veterinary Association Gastrointestinal Standardization Group. Journal of comparative pathology, 138 Suppl 1: 1-43.

Evans SE, Bonczynski JJ, Broussard JD, Han E, Baer KE. 2006. Comparison of endoscopic and full-thickness biopsy specimens for diagnosis of inflammatory bowel disease and alimentary tract lymphoma in cats. Journal of the American Veterinary Medical Association, 229 (9): 1447–1450.

Gieger T. 2011. Alimentary lymphoma in cats and dogs. The veterinary clinics of North America. Small animal practice, 41 (2): 419–432.

Gress V, Wolfesberger B, Fuchs-Baumgartinger A, Nedorost N, Saalmüller A, Schwendenwein I, Rütgen BC, Hammer SE. 2016. Characterization of the T-cell receptor gamma chain gene rearrangements as an adjunct tool in the diagnosis of T-cell lymphomas in the gastrointestinal tract of cats. Research in veterinary science, 107: 261–266.

Habtezion A, Nguyen LP, Hadeiba H, Butcher EC. 2016. Leukocyte trafficking to the small intestine and colon. Gastroenterology, 150 (2): 340–354.

Hammer SE, Groiss S, Fuchs-Baumgartinger A, Nedorost N, Gress V, Luckschander-Zeller N, Saalmüller A, Schwendenwein I, Rütgen BC. 2017. Characterization of a PCR-based lymphocyte clonality assay as a complementary tool for the diagnosis of feline lymphoma. Veterinary and comparative oncology, 15 (4): 1354–1369.

Hardy WD. 1981. Hematopoietic tumors of cats. Journal of the American Animal Hospital Association, 1981 (17): 921–940.

Jergens AE. 1999. Inflammatory bowel disease. Current perspectives. The veterinary clinics of North America. Small animal practice, 29 (2): 501-21, vii.

Jergens AE. 2012. Feline idiopathic inflammatory bowel disease: what we know and what remains to be unraveled. Journal of feline medicine and surgery, 14 (7): 445–458.

Jergens AE, Moore FM, Haynes JS, Miles KG. 1992. Idiopathic inflammatory bowel disease in dogs and cats: 84 cases (1987-1990). Journal of the American Veterinary Medical Association, 201 (10): 1603–1608.

Keller SM, Vernau W, Moore PF. 2016. Clonality testing in veterinary medicine: A review with diagnostic guidelines. Veterinary pathology, 53 (4): 711–725.

Kiupel M, Smedley RC, Pfent C, Xie Y, Xue Y, Wise AG, DeVaul JM, Maes RK. 2011. Diagnostic algorithm to differentiate lymphoma from inflammation in feline small intestinal biopsy samples. Veterinary pathology, 48 (1): 212–222.

Konno A, Hashimoto Y, Kon Y, Sugimura M. 1994. Perforin-like immunoreactivity in feline globule leukocytes and their distribution. The journal of veterinary medical science, 56 (6): 1101–1105.

Langerak AW, Groenen PJTA, Brüggemann M, Beldjord K, Bellan C, Bonello L, Boone E, Carter GI, Catherwood M, Davi F, Delfau-Larue M-H, Diss T, Evans PAS, Gameiro P, Garcia Sanz R, Gonzalez D, Grand D, Håkansson A, Hummel M, Liu H, Lombardia L, Macintyre EA, Milner BJ, Montes-Moreno S, Schuuring E, Spaargaren M, Hodges E, van Dongen JJM. 2012. EuroClonality/BIOMED-2 guidelines for interpretation and reporting of Ig/TCR clonality testing in suspected lymphoproliferations. Leukemia, 26 (10): 2159–2171.

Liebich H-G, Budras K-D. 2010. Funktionelle Histologie der Haussäugetiere und Vögel. Lehrbuch und Farbatlas für Studium und Praxis. Fünfte Auflage. Stuttgart: Thieme Verlagsgruppe.

Lingard AE, Briscoe K, Beatty JA, Moore AS, Crowley AM, Krockenberger M, Churcher RK, Canfield PJ, Barrs VR. 2009. Low-grade alimentary lymphoma: Clinicopathological findings and response to treatment in 17 cases. Journal of feline medicine and surgery, 11 (8): 692–700.

Louwerens M, London CA, Pedersen NC, Lyons LA. 2005. Feline lymphoma in the post–feline leukemia virus era. Journal of veterinary internal medicine, 19 (3): 329.

Luckschander-Zeller N, Hammer SE, Ruetgen BC, Tichy A, Thalhammer JG, Haas E, Richter B, Welle M, Burgener IA. 2019. Clonality testing as complementary tool in the assessment of different patient groups with canine chronic enteropathy. Veterinary immunology and immunopathology, 214.

Mahony OM, Moore AS, Cotter SM, Engler SJ, Brown D, Penninck DG. 1995. Alimentary lymphoma in cats: 28 cases (1988-1993). Journal of the American Veterinary Medical Association, 207 (12): 1593–1598.

Marsilio S, Ackermann MR, Lidbury JA, Suchodolski JS, Steiner JM. 2019b. Results of histopathology, immunohistochemistry, and molecular clonality testing of small intestinal biopsy specimens from clinically healthy client-owned cats. Journal of veterinary internal medicine, 33 (2): 551–558.

Marsilio S, Newman SJ, Estep JS, Giaretta PR, Lidbury JA, Warry E, Flory A, Morley PS, Smoot K, Seeley EH, Powell MJ, Suchodolski JS, Steiner JM. 2020. Differentiation of

lymphocytic-plasmacytic enteropathy and small cell lymphoma in cats using histology-guided mass spectrometry. Journal of veterinary internal medicine, 34 (2): 669–677.

Marsilio S, Pilla R, Sarawichitr B, Chow B, Hill SL, Ackermann MR, Estep JS, Lidbury JA, Steiner JM, Suchodolski JS. 2019a. Characterization of the fecal microbiome in cats with inflammatory bowel disease or alimentary small cell lymphoma. Scientific reports, 9 (1).

Mochizuki H, Nakamura K, Sato H, Goto-Koshino Y, Sato M, Takahashi M, Fujino Y, Ohno K, Uchida K, Nakayama H, Tsujimoto H. 2011. Multiplex PCR and Genescan analysis to detect immunoglobulin heavy chain gene rearrangement in feline B-cell neoplasms. Veterinary immunology and immunopathology, 143 (1-2): 38–45.

Mochizuki H, Nakamura K, Sato H, Goto-Koshino Y, Sato M, Takahashi M, Fukushima K, Nakashima K, Fujino Y, Ohno K, Uchida K, Nakayama H, Tsujimoto H. 2012. GeneScan analysis to detect clonality of T-cell receptor γ gene rearrangement in feline lymphoid neoplasms. Veterinary immunology and immunopathology, 145 (1-2): 402-409.

Moore PF, Rodriguez-Bertos A, Kass PH. 2012. Feline gastrointestinal lymphoma: Mucosal architecture, immunophenotype, and molecular clonality. Veterinary pathology, 49 (4): 658–668.

Moore PF, Woo JC, Vernau W, Kosten S, Graham PS. 2005. Characterization of feline T cell receptor gamma (TCRG) variable region genes for the molecular diagnosis of feline intestinal T cell lymphoma. Veterinary immunology and immunopathology, 106 (3-4): 167–178.

Paulin MV, Couronné L, Beguin J, Le Poder S, Delverdier M, Semin M-O, Bruneau J, Cerf-Bensussan N, Malamut G, Cellier C, Benchekroun G, Tiret L, German AJ, Hermine O, Freiche V. 2018. Feline low-grade alimentary lymphoma: An emerging entity and a potential animal model for human disease. BMC veterinary research, 14 (1): 306.

Pohlman LM, Higginbotham ML, Welles EG, Johnson CM. 2009. Immunophenotypic and histologic classification of 50 cases of feline gastrointestinal lymphoma. Veterinary pathology, 46 (2): 259–268.

QIAGEN GmbH. 2017. https://www.pipety.cz/data/machines/hb-0804-010_1108754_um_ias_qx_advanced_1117_ww.pdf (accessed Nov 14, 2020).

Rezuke WN, Abernathy EC, Tsongalis GJ. 1997. Molecular diagnosis of B- and T-cell lymphomas: Fundamental principles and clinical applications. Clinical chemistry, 43 (10): 1814–1823.

Roccabianca P, Woo JC, Moore PF. 2000. Characterization of the diffuse mucosal associated lymphoid tissue of feline small intestine. Veterinary immunology and immunopathology, 75 (1-2): 27–42.

Rout ED, Burnett RC, Yoshimoto JA, Avery PR, Avery AC. 2019. Assessment of immunoglobulin heavy chain, immunoglobulin light chain, and T-cell receptor clonality testing in the diagnosis of feline lymphoid neoplasia. Veterinary clinical pathology, 48 Suppl 1: 45–58.

Sabattini S, Bottero E, Turba ME, Vicchi F, Bo S, Bettini G. 2016. Differentiating feline inflammatory bowel disease from alimentary lymphoma in duodenal endoscopic biopsies. The journal of small animal practice, 57 (8): 396–401.

Unterkreuter S, Posautz A, Rütgen BC, Groiss S, Kübber-Heiss A, Hammer SE. 2020. First-time application of a PCR-based clonality assay in a large cohort of non-domestic felines. Research in veterinary science.

Uzal FA, Plattner BL, Hostetter JM. 2016. Alimentary System. In: Maxie MG, ed. Jubb, Kennedy, and Palmer's pathology of domestic animals. Volume 2. Sixth edition. St. Louis, Missouri: Elsevier, 1-257.e2.

Vail DM, Moore AS, Ogilvie GK, Volk LM. 1998. Feline lymphoma (145 cases): Proliferation indices, cluster of differentiation 3 immunoreactivity, and their association with prognosis in 90 cats. Journal of veterinary internal medicine, 12 (5): 349–354.

Valli VE, Jacobs RM, Parodi A. 2002. Histological classification of hematopoietic tumors of domestic animals. Armed forces institute of pathology, 2002 (2nd Series Vol. VIII).

Washabau RJ, Day MJ, Willard MD, Hall EJ, Jergens AE, Mansell J, Minami T, Bilzer TW. 2010. Endoscopic, biopsy, and histopathologic guidelines for the evaluation of gastrointestinal inflammation in companion animals. Journal of veterinary internal medicine, 24 (1): 10–26.

9. List of figures and tables

10. Appendix

Table 6: Age of samples, T-cell clonality results, layer-associated categories of lymphoplasmacytic infiltration based on histopathology and immunohistochemistry and results of immunohistochemistry.

		T-cell clonality				
		TCRG-J1	TCRG-J2	**clonality**		**estimated ratio of**
case ID	**date**	approx. 100 bp	approx. 100 bp	**result**	**categories based on histopathology and immunohistochemistry**	**T:B lymphocytes (immonhistochemistry)**
2	2018	pc	pc	n/d	mild lymphoplasmacytic infiltration of the Lamina propria mucosae	50/50
3	2017	pc	pc	n/d	mild lymphoplasmacytic infiltration of the Lamina propria mucosae	50/50
4	2017	pc	pc	n/d	mild lymphoplasmacytic infiltration of the Lamina propria mucosae	50/50
7	2016	pc	pc	n/d	mild lymphoplasmacytic infiltration of the Lamina propria mucosae	50/50
9	2016	bc	mc	T-cell	mild lymphoplasmacytic infiltration of the Lamina propria mucosae	90/10
11	2015	pc	pc	n/d	mild lymphoplasmacytic infiltration of the Lamina propria mucosae	50/50
12	2015	pc	pc	n/d	mild lymphoplasmacytic infiltration of the Lamina propria mucosae	50/50
14	2014	mc	oc	T-cell	mild lymphoplasmacytic infiltration of the Lamina propria mucosae	50/50
15	2014	pc	pc	n/d	mild lymphoplasmacytic infiltration of the Lamina propria mucosae	50/50
16	2014	pc	pc	n/d	mild lymphoplasmacytic infiltration of the Lamina propria mucosae	50/50
21	2013	pc	mc(+bg)	T-cell	mild lymphoplasmacytic infiltration of the Lamina propria mucosae	60/40
24	2012	psc	mc	T-cell	mild lymphoplasmacytic infiltration of the Lamina propria mucosae	50/50
29	2007	oc	mc	T-cell	mild lymphoplasmacytic infiltration of the Lamina propria mucosae	50/50
31	2007	pc	mc	T-cell	mild lymphoplasmacytic infiltration of the Lamina propria mucosae	50/50
32	2007	bc	mc	T-cell	mild lymphoplasmacytic infiltration of the Lamina propria mucosae	60/40
22	2013	mc	mc	T-cell	mild lymphoplasmacytic infiltration of the Lamina propria mucosae and the Tela submucosa	60/40
13	2014	pc	pc	n/d	mild lymphoplasmacytic infiltration of the Lamina propria mucosae and the Tela submucosa	60/40
18	2013	mc	mc	T-cell	mild lymphoplasmacytic infiltration of the Lamina propria mucosae and the Tela submucosa	90/10
19	2013	pc	mc	T-cell	mild lymphoplasmacytic infiltration of the Lamina propria mucosae and the Tela submucosa	70/30

23	2012	bc	bc	T-cell	mild lymphoplasmacytic infiltration of the Lamina propria mucosae and the Tela submucosa	50/50
25	2011	mc(+bg)	mc(+bg)	T-cell	mild lymphoplasmacytic infiltration of the Lamina propria mucosae and the Tela submucosa	50/50
27	2010	bc	bc	T-cell	mild lymphoplasmacytic infiltration of the Lamina propria mucosae and the Tela submucosa	90/10
1	2018	mc(+bg)	oc	T-cell	moderate lymphoplasmacytic infiltration of the Lamina propria mucosae	60/40
5	2017	mc(+bg)	psc	T-cell	moderate lymphoplasmacytic infiltration of the Lamina propria mucosae	50/50
17	2014	pc	bc	T-cell	moderate lymphoplasmacytic infiltration of the Lamina propria mucosae	80/20
26	2012	psc	psc	n/d	moderate lymphoplasmacytic infiltration of the Lamina propria mucosae	60/40
28	2008	mc	mc	T-cell	moderate lymphoplasmacytic infiltration of the Lamina propria mucosae	50/50
30	2007	mc(+bg)	mc(+bg)	T-cell	moderate lymphoplasmacytic infiltration of the Lamina propria mucosae	50/50
33	2007	bc	bc	T-cell	moderate lymphoplasmacytic infiltration of the Lamina propria mucosae	50/50
6	2016	mc(+bg)	mc(+bg)	T-cell	moderate lymphoplasmacytic infiltration of the Lamina propria mucosae and the Tela submucosa	50/50
8	2016	mc(+bg)	pc	T-cell	moderate lymphoplasmacytic infiltration of the Lamina propria mucosae and the Tela submucosa	90/10
10	2015	pc	mc(+bg)	T-cell	moderate lymphoplasmacytic infiltration of the Lamina propria mucosae and the Tela submucosa	60/40
20	2013	mc	mc	T-cell	moderate lymphoplasmacytic infiltration of the Lamina propria mucosae and the Tela submucosa	60/40
34	2007	psc	psc	n/d	moderate lymphoplasmacytic infiltration of the Lamina propria mucosae and the Tela submucosa	90/10

bc: biclonal, mc: monoclonal, mc+bg: monoclonal with background, n/d: not detected, oc: oligoclonal, pc: polyclonal, psc: pseudoclonal